

ABSTRACT

Glioblastoma (GBM), the most common and malignant primary brain tumor, is currently incurable and the most recent advance in treatment yields a median survival of only 12-15 months.¹⁻³ To account for GBM's heterogeneity, molecular diagnostics may be used to enable mutation specific treatment and improve patient outcomes.⁴ Mutations in *PIK3CA*, the p110 α subunit of phosphatidylinositide 3-kinase (PI3K), are important in pathogenesis of other cancers, and drugs targeting PI3K are in clinical development.⁵⁻⁸ In 12% of GBM, *PIK3CA* is mutated and recurrent mutations are distributed across three functional domains (adaptor-binding, helical, and kinase).⁶ As their role in GBM tumorigenesis is unknown, we examined six mutations known to occur in GBM, two per mutated domain, for activation of biochemical signaling through phosphorylation of downstream targets ATK and S6. These mutations were introduced into immortalized human astrocytes, with and without oncogenic RAS.⁹ We determined that the downstream signaling molecule AKT is activated by all of the mutations in human astrocytes, with the greatest increase caused by mutations in the helical and kinase domains. The presence of oncogenic RAS cooperated with the helical and kinase domain mutations to activate signaling. Mutations in the adaptor-binding domain appear to increase signaling independently of oncogenic RAS. Mutations in *PIK3CA* therefore differentially increase signaling, leading to differing phenotypes and possible differential response to PI3K inhibitors. By understanding the consequences of differing mutations, GBM diagnosis and treatment can be improved.

INTRODUCTION

Class I phosphatidylinositide 3-kinases (PI3K) are activated by receptor tyrosine kinases (RTK) and have an established role in cancer biology, making them an important target for research and drug development.¹⁰ In general, phosphatidylinositide 3-kinase proteins form a diverse family of related enzymes, whose members are divided into three classes based on their structural features and lipid substrates.^{8, 11} Class II and III members do not have a well-established role in cancer, however signaling by Class I members has been shown to promote cellular survival, proliferation, and migration, along with other hallmarks of cancer.^{5, 8, 11, 12} These proteins are heterodimeric, with our focus being on the catalytic subunit encoded by *PIK3CA* and the regulatory subunit encoded by *PIK3R1* due to their frequent mutation in cancer.⁶ The catalytic subunit produces a phosphatidylinositol-3,4,5-triphosphate (PIP₃) secondary messenger from membrane bound phosphatidylinositol-4,5-bisphosphate (PIP₂) and the regulatory subunit inhibits this activity. There are many upstream signals interacting specifically with each subunit, and the ability of these signals to activate signaling depends on the catalytic isoform present in the heterodimer.^{8, 11, 13}

In GBM, three PI3K pathway genes are frequently mutated: *PIK3CA* (12%) (Fig. 1A), *PIK3R1* (12%), and *PTEN* (41%).^{5, 14, 15} These mutations are mutually exclusive, suggesting that they all activate PI3K signaling and that a mutation in one is sufficient to promote tumorigenesis. Mutations in *PIK3R1* and *PTEN* have been shown to be transformative in brain tissue, and although *PIK3CA* mutations are presumed to drive gliomagenesis based on mutational frequency and established role in other cancers, this has not yet been investigated experimentally.⁶ Crosstalk between pathways occurs, leading us to investigate the influence of

the oncogene RAS from the mitogen-activated protein kinase (MAPK) arm of the RTK pathway (Fig. 1B). PIK3CA mutations in GBM are spread across the protein, with recurring mutations in the helical, kinase, and adaptor binding (ABD) domains (Fig. 1C, 1D).⁷ The helical (E542K and E545K) and kinase (H1047R) domain mutations have been shown to initiate tumorigenesis and promote progression in non-brain tissues, such as breast.¹⁶⁻¹⁸ Structural analysis has been used to predict the mechanisms of mutations in these three domains.^{13, 19-23} Helical domain mutations are predicted to disrupt inhibitory interactions between PIK3R1 and PIK3CA, leading to signaling activation. Kinase domain mutations are predicted to alter the conformation of the PIK3CA protein's activation loop, resulting in increased binding to the cellular membrane and therefore increased catalytic efficiency. ABD mutations are predicted to alter the conformation of the kinase domain, leading to an increase in the protein's enzymatic activity. Helical domain mutations have been found to require RAS for signaling activation but not PIK3R1 in non-brain models, whereas the opposite is true for kinase domain mutations.²⁴ The role of RAS and PIK3R1 is unclear for ABD mutations.

To determine if PIK3CA mutations differentially activate PI3K signaling based on the mutated domain, we selected six specific mutations known to occur in GBM (R88Q, C90Y, E542K, E545K, M1043V, and H1047R) (Fig. 1D) and introduced them into immortalized astrocytes with and without oncogenic RAS. The use of cultured genetically engineered cells has important advantages over other preclinical models, as they allow direct genotype to phenotype conclusions.^{9, 25} These cells are also more experimentally manageable, and can be used for *in vitro* and *in vivo* evaluation (through intracranial transplantation). The mutations were therefore introduced into human astrocytes (NHA), which have been immortalized by

expressing the HPV oncogenes E6 and E7 to inhibit the TP53 and RB pathways and expression of hTERT for telomere maintenance.⁹ These genetic modifications are required for culture of astrocytes, but do not transform the cells or make them tumorigenic.⁹ The mutations were also introduced into astrocytes that express oncogenic HRAS (NHARAS), as a way to examine effects between the PI3K and MAPK effector arms of the RTK pathway.⁹ Both of these effector arms are frequently mutated and activated in GBM.⁶ We propose that signaling activation is dependent not only on the specific gene that is mutated but also on the precise location within the mutated protein. Even though mutations in all three functional domains of PIK3CA are assumed to activate signaling, drive tumor growth, and predict PI3K inhibitor activity, none of these assumptions has yet been successfully experimentally tested. The validity of these mechanisms must be proven to provide a rational basis for developing individualized therapy.

MATERIALS AND METHODS

Tissue Culture

Immortalized normal human astrocytes (NHA) with and without oncogenic H-RAS were a gift from Dr. Russell O. Pieper.⁹ All cell lines were maintained in Dulbecco's Modified Eagle's Medium supplemented with 10% FBS and 1% Penn/Strep (complete DMEM) at 37°C and 5% CO₂.

PIK3CA Mutagenesis

HA-tagged wildtype PIK3CA (PIK3CA^{wt}, pBABE-puro-HAPIK3CA), HA-tagged GFP (GFP, pDEST-Flag-HA-GFP), pENTR4 vector (pENTR4-no-ccDB), and third generation lentiviral Gateway destination vector (pLenti-PGK-Hygro-DEST) plasmids were purchased from Addgene (Cambridge, MA). PIK3CA^{wt} and GFP genes were excised using restriction digests and inserted

via ligation into the pENTR4 vector. Point mutagenesis of *PIK3CA* was performed in the pENTR4 vector using the Q5 Site-Directed Mutagenesis Kit (New England Biolabs, Ipswich, MA) according to manufacturer's instructions generating the six *PIK3CA* mutants (*PIK3CA*^{mut}: R88Q, C90Y, E542K, E545K, M1043V, H1047R). The sequence of each mutated gene was confirmed with Sanger sequencing (Genewiz, South Plainfield, NJ). Each gene (GFP, *PIK3CA*^{wt}, and six *PIK3CA*^{mut}) was transferred from the pENTR4 vector to the pLenti-PGK-Hygro-DEST vector by recombination as previously described.²⁶

Lentivirus Production

Lentiviral particles containing GFP, *PIK3CA*^{wt}, or individual *PIK3CA*^{mut} were generated using 293FT cells (Invitrogen, Grand Island, NY). Briefly, 5×10^5 cells were plated on 10 cm plates in complete DMEM supplemented with 2 mM GlutaMAX (Invitrogen), 0.1 mM MEM Non-Essential Amino Acids (Invitrogen), and 1 mM sodium pyruvate (Invitrogen) (293FT medium). The next day medium was replaced with fresh 293FT medium without Penn/Strep, and with 9 μ g GFP, *PIK3CA*^{wt}, or *PIK3CA*^{mut} pDEST vector plasmids, 9 μ g pLP1, 3.6 μ g pLP, and 1.89 μ g pMD2.G transfected into these cells using Lipofectamine 2000 (Invitrogen) according to the manufacturer's instructions. After 24 hours, medium was exchanged for new 293FT medium supplemented with 1 M HEPES (Invitrogen). At 48 and 72 hours post-transfection, viral supernatants were collected and fresh 293FT medium supplemented with 1M HEPES was added. Viral supernatants from each time point were filtered through a 45 μ m PES filter, and stored at 4°C until all time points could be pooled, aliquoted, and stored at -80°C.

Creation of Stable Cell Lines

NHA and NHARAS cells were plated at 135,000 and 120,000 cells per plate on 6 cm plates and infected with lentiviral particles after two days. Viral particles and cells were incubated overnight in complete DMEM containing 8 µg/ml polybrene (Sigma-Aldrich, St. Louis, MO) at 37°C and 5% CO₂. Two days post-infection, transduced cells were selected by culture in complete DMEM with 300 µg/ml hygromycin B for 14 days. Stable gene expression was confirmed by immunoblot for the HA tag on GFP, PIK3CA^{wt} and PIK3CA^{mut}.

Immunoblot

NHA and NHARAS cells were serum starved in 0.5% FBS for 24 hours, harvested, lysed, and quantified by BCA (Pierce BCA Protein Assay Kit, Thermo Scientific, Waltham, MA). Protein samples (20 µg) were separated by gradient (8-16%) SDS-PAGE (Bio-Rad, Hercules, CA) and transferred to PDVF membranes (EMD Millipore Corp, Billerica, MA). The membranes were probed with primary antibodies against GAPDH (EMD Millipore Corp, Billerica, MA, MAB374) at 1:7000, AKT (Cell Signaling Technology, Danvers, MA, CST2920S) at 1:3000, phospho AKT (Ser473) (Cell Signaling Technology, Danvers, MA, CST4060) at 1:3000, phospho S6 (Ser240/244) (Cell Signaling Technology, Danvers, MA, CST2215) at 1:3000, ERK (Cell Signaling Technology, Danvers, MA, CST4696) at 1:3000, and phospho ERK (Thr202/Tyr204) (Cell Signaling Technology, Danvers, MA, CST4370) at 1:3000. Blots were probed with Alexa 488, 555, or 647 conjugated secondary antibodies (Life Technologies, Grand Island, NY) and imaged on a Typhoon Trio (GE Healthcare, Pittsburgh, PA). To detect HA-tagged proteins, membranes were probed separately with an anti-HA-peroxidase antibody (Roche Applied Science, Penzberg, Germany, 12013819001) at 1:1000, and imaged using enhanced chemiluminescence (Clarity

Western ECL Substrate, Bio-Rad) on an Image Quant LAS 4000 (GE Healthcare). Immunoblot images were analyzed using ImageJ (NIH, Bethesda, MD), normalized to GAPDH, normalized to an external standard, and expression levels were set relative to parental, uninfected cells. Immunoblots were performed with 1 (NHA) and 3 – 4 (NHARAS) experimental replicates. Differences between cell lines were determined by one-way ANOVA tests using Tukey’s post-tests for multiple comparisons in GraphPad Prism 5 (La Jolla, CA). For statistical analysis P values < 0.05 were considered to be significant.

RESULTS

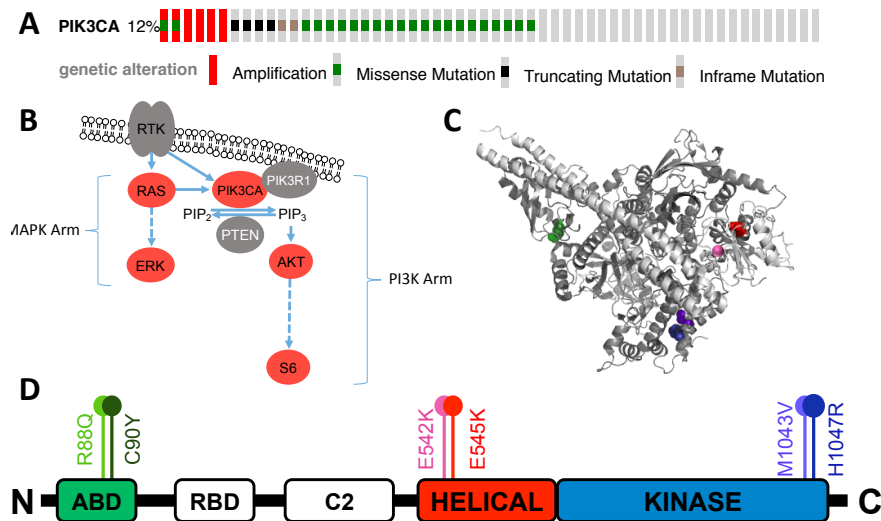


Figure 1: PIK3CA mutations in GBM. (A) Occurrence of PIK3CA mutations in a sampling of 273 GBM patients, courtesy of cBioPortal.¹⁴ (B) Abbreviated figure of the MAPK and PI3K arms of the RTK pathway, proteins examined in this paper are red, and dashed lines indicate multiple steps. (C) PyMOL (Schrödinger, New York City, NY) generated protein model with mutation locations marked. (D) Simplified protein diagram showing mutation locations within protein domains, R88Q and M1043V are rare mutations, C90Y is unique to GBM, and E542K, E545K and H1047R are “hot-spot” mutations seen in other cancers.

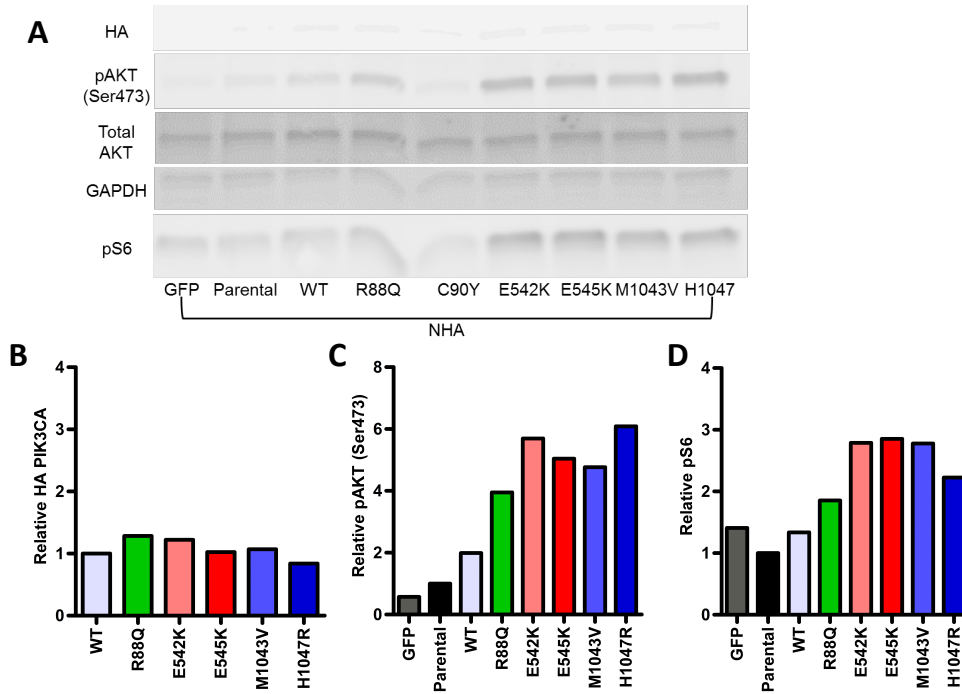


Figure 2: PI3K signaling in *PIK3CA* mutant NHA (A) Immunoblot of cell lysates probed for the HA tagged *PIK3CA*, phosphorylated AKT, total AKT, GAPDH (loading control), and phosphorylated S6 (B) Plot of HA levels relative to *PIK3CA*^{wt}. (C) Plot of pAKT levels relative to parental NHAs. (D) Plot of pS6 levels relative to parental NHAs.

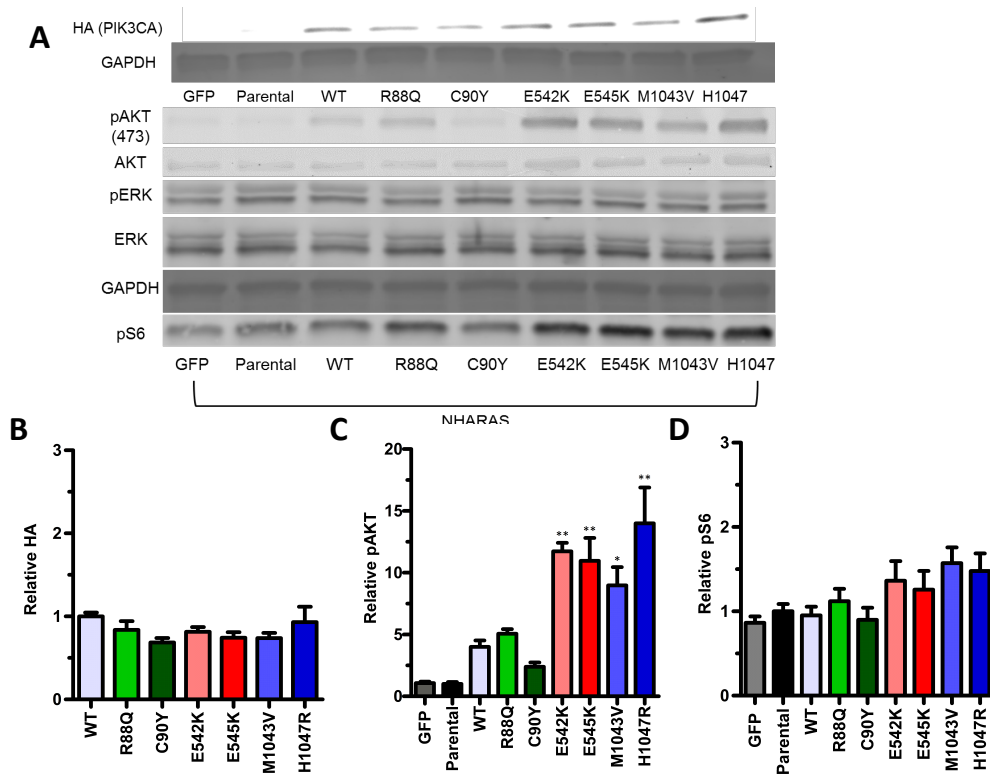


Figure 3: PI3K signaling in *PIK3CA* mutant NHARAS. (A) Immunoblot of cell lysates probed for HA tag, phosphorylated AKT, total AKT, phosphorylated ERK, total ERK, GAPDH (loading control), and phosphorylated S6. (B) Plot of HA levels relative to *PIK3CA*^{wt}. (C) Plot of pAKT levels relative to parental. (D) Plot of pS6 levels relative to parental. (*) dictates significant difference from parental and (**) dictates significant difference from *PIK3CA*^{wt}.

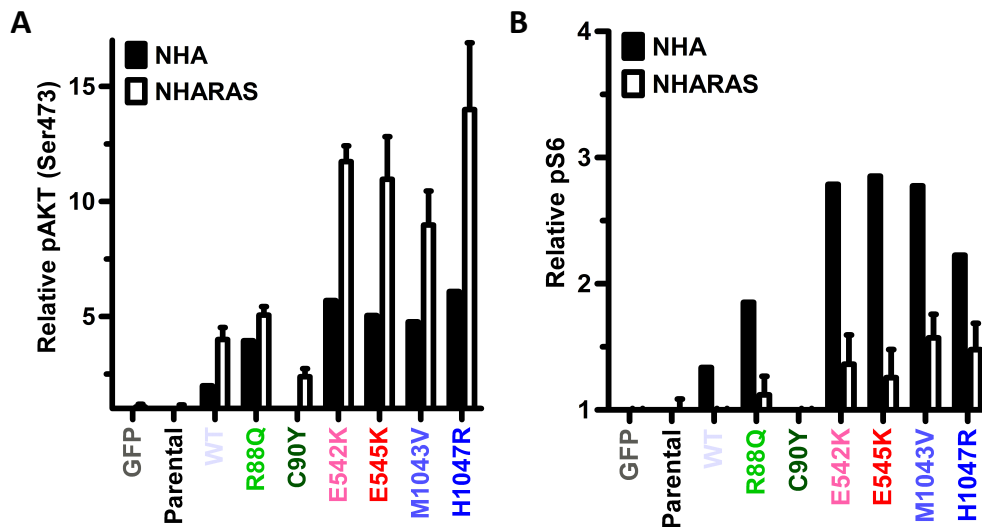


Figure 4: Comparison of phosphorylated AKT and phosphorylated S6 between NHA and NHARAS cells. (A) Plot of pAKT in NHA and NHARAS relative to parental cells. (B) Plot of pS6 in NHA and NHARAS relative to parental cells.

As *PIK3CA* mutations are seen in 12% of GBM (Fig. 1A), we introduced six mutations into genetically engineered human astrocytes in the presence and absence of oncogenic RAS to determine their impact on PI3K signaling (Fig. 1B) and gliomagenesis. These mutations were distributed across three functionally distinct domains, with two mutations per domain and including several “hot-spot mutations” that commonly occur and are transformative in other cancers (Fig. 1C, 1D).¹⁶⁻¹⁸

PIK3CA mutations affected signaling to different degrees, based the specific amino acid that is mutated. We confirmed expression of the *PIK3CA* mutations in NHA by immunoblotting for HA (Fig. 2A, 2B). HA levels were approximately equal across *PIK3CA*^{wt} and *PIK3CA*^{mut} indicating that any observed signaling differences were due to the mutation, not differences in engineered protein levels. PI3K signaling activation was measured through phosphorylation of AKT and the more downstream target S6. Expression of the *PIK3CA* plasmids did not alter total AKT levels (Fig. 2A). Cells with GFP insertion do not show a pAKT increase compared to parental,

confirming that viral transduction did not alter PI3K signaling. PIK3CA^{wt} increased pAKT signaling two fold compared to parental, showing a slight increase due to increased levels of PIK3CA protein (Fig. 2C). The ABD mutation, R88Q, increased pAKT four times as much as parental and twice as much as PIK3CA^{wt}, but helical and kinase domain mutations produced a greater increase in signaling (Fig. 2C). E542K and H1047R show a six-fold increase compared to parental and about a three-fold increase compared to PIK3CA^{wt} (Fig. 2C). E545K and M1043V show about a five-fold increase compared to parental and more than double levels seen in PIK3CA^{wt} (Fig. 2C). The more distal signaling molecule pS6 shows a similar trend but with more minor increases (Fig. 2D). PIK3CA^{wt} only increased signaling by 25% relative to parental, while R88Q has about a two-fold increase and E542K, E545K, and M1043V show about a three-fold increase in pS6 (Fig. 2D). GFP has an increase similar to that of PIK3CA^{wt}, however this could also be due to experimental error, and more biological replicates are needed to confirm these results.

Because RAS has been shown to differentially influence the effects of PIK3CA mutations in non-neural tissues, we wanted to determine whether the presence of oncogenic RAS influences PI3K signaling in PIK3CA mutant astrocytes. Therefore, we introduced the six mutations into NHARAS. In the generated NHARAS cell lines, the presence of our engineered PIK3CA protein was confirmed by HA probing (Fig. 3A). There were no significant differences in relative HA levels between cell lines showing equivalent levels of expression (Fig. 3A, 3B). Similar to NHAs, the relative amounts of pAKT differed with mutation, though total AKT levels were constant (Fig. 3A). PIK3CA^{wt} increased pAKT levels four-fold over parental NHARAS, while R88Q increased pAKT by five-fold (Fig. 3C). The C90Y mutation only increased signaling by about

two-fold compared to parental, suggesting that it is a less potent activator of PI3K signaling than PIK3CA^{wt} (Fig. 3C). The helical and kinase domain mutations had more dramatic increases, with E542K and E545K showing a 12-fold increase from parental and a significant two-fold increase over PIK3CA^{wt} (Fig. 3C). Kinase mutant M1043V shows about an eight-fold increase with statistical difference from parental, and around a two-fold increase from PIK3CA^{wt} (Fig. 3C). H1047R shows the greatest increase at about 13 times that of parental and shows over a three-fold increase and statistical difference from PIK3CA^{wt} (Fig. 3C). Changes in levels of pS6 were less dramatic, with R88Q and C90Y showing levels similar to parental and PIK3CA^{wt} (Fig. 3D). The helical and kinase domain mutants show a slightly greater increase, but only reach about 1.5 times parental levels (Fig. 3D).

To determine the effects of oncogenic RAS in PI3KCA mutant astrocytes by we compared PI3K signaling in its presence and absence. In the absence of oncogenic RAS, pAKT increases are apparent but pS6 increases are less pronounced (Fig 4A, 4B). The presence of oncogenic RAS yields much greater increases in proximal signaling through pAKT seen by the over 10-fold increases compared to parental from helical and kinase mutants (Fig. 4A). In contrast, more distal signaling through pS6 shows a less dramatic result compared to parental (Fig. 4B).

DISCUSSION

By understanding how PIK3CA mutations activate signaling and promote tumorigenesis, we may better comprehend the genetic drivers of GBM and how to combat them with molecularly targeted inhibitors. As mutations may influence cellular behavior differently, they may not respond equivalently to inhibitors and would therefore require differential treatments.

The ability to interpret the function and variation between these mutations is fundamental to the goal of improving treatment and increasing patient survival.

PIK3CA mutations differentially influence signaling, and responses are influenced by the presence of oncogenic RAS. As all mutants tested except for C90Y increase signaling beyond levels seen from overexpression of PIK3CA^{wt}, they are activating; however the location of the mutation within the protein is important for the extent of activation. The helical and kinase domain mutations are the most activating, though R88Q is also activating in NHAs. This activation continues down the pathway as it is still seen in increased levels of pS6, but increases are less dramatic likely due to translation downstream. This suggests that R88Q, and the helical and kinase domain mutations promote tumorigenesis by increasing signaling down the PI3K pathway. In the presence of oncogenic RAS, helical and kinase domain mutations dramatically increase pAKT signaling, suggesting that oncogenic RAS cooperates with the helical mutations to promote AKT activation. This increase also suggests that H1047R activity is influenced by oncogenic RAS despite previous evidence that it functions independently of RAS binding.^{20, 24} The adaptor binding domain mutation R88Q shows only a slight increase compared to PIK3CA^{wt}, and C90Y shows a decrease in signaling suggesting that this mutation leads to decreased activity of PIK3CA. The similar levels of pAKT in R88Q mutants in the presence and absence of RAS suggests that the presence of oncogenic RAS does not influence its ability to activate PI3K signaling. Increases in pS6 are much less dramatic, however this could be due to the already higher baseline levels of pS6 in the presence of oncogenic RAS.

The transformative effects of the helical and kinase mutations along with R88Q in the absence of oncogenic RAS suggests that inhibition of PI3K in *PIK3CA* mutant GBM may be a

promising therapeutic option. Increases in signaling seen by phosphorylation of AKT and S6 would be predicted to lead to increases in proliferation and migration. We have seen that this is indeed the case, as increased signaling caused by these mutations translates into phenotypic consequences such as proliferation, migration, and tumorigenesis *in vivo* (data not shown). This suggests that PI3KCA mutations in the helical and kinase domains are transformative, and promote gliomagenesis. Understanding differences between mutations is critical to predicting the biology of patient tumors. Mutations that promote tumorigenesis may not respond well to PI3K inhibitors, therefore understanding the responses of various mutations is necessary for directed patient treatment. Future studies investigating the response of these mutations to PI3K inhibitors will make progress towards mutation based diagnosis and increased efficacy in treatment.

ACKNOWLEDGEMENTS

Thanks to Robbie McNeill, Demi Canoutas, Ralf Schmid, Ryan Bash, and Dr. C. Ryan Miller.

This research was funded in part by a Summer Undergraduate Research Fellowship from the Office for Undergraduate Research at the University of North Carolina at Chapel Hill.

This research was funded by a NC TraCS grant.

LITERATURE CITED

- 1) Stupp, R.; Mason, W. P.; Van Den Bent, M. J.; Weller, M.; Fisher, B.; Taphoorn, M. J.; Belanger, K.; Brandes, A. A.; Marosi, C.; Bogdahn, U.; Curschmann, J.; Janzer, R. C.; Ludwin, S. K.; Gorlia, T.; Allgeier, A.; Lacombe, D.; Cairncross, J. G.; Eisenhauer, E.; Mirimanoff, R. O.; European Organisation for R.; Treatment of Cancer Brain T.; Radiotherapy G.; National Cancer Institute of Canada Clinical Trials G. Radiotherapy plus concomitant and adjuvant temozolomide for glioblastoma. *N. Engl. J. Med.* **2005**, 352, 987-96.
- 2) Ostrom, Q. T.; Gittleman, H.; Farah, P.; Ondracek, A.; Chen, Y.; Wolinsky, Y.; Stroup, N. E.; Kruchko, C.; Barnholtz-Sloan, J. S. CBTRUS statistical report: Primary brain and central nervous system tumors diagnosed in the United States in 2006-2010. *Neuro. Oncol.* **2013**, 15 Suppl 2, ii1-56.

- 3) Stupp, R.; Hegi, M. E.; Mason, W. P.; Van Den Bent, M. J.; Taphoorn, M. J.; Janzer, R. C.; Ludwin, S. K.; Allgeier, A.; Fisher, B.; Belanger, K.; Hau, P.; Brandes, A. A.; Gijtenbeek, J.; Marosi, C.; Vecht, C. J.; Mokhtari, K.; Wesseling, P.; Villa, S.; Eisenhauer, E.; Gorlia, T.; Weller, M.; Lacombe, D.; Cairncross, J. G.; Mirimanoff, R. O.; European Organisation for R.; Treatment of Cancer Brain T.; Radiation Oncology G.; National Cancer Institute of Canada Clinical Trials G. Effects of radiotherapy with concomitant and adjuvant temozolomide versus radiotherapy alone on survival in glioblastoma in a randomised phase III study: 5-year analysis of the EORTC-NCIC trial. *Lancet. Oncol.* **2009**, *10*, 459-66.
- 4) Mendelsohn, J. Personalizing oncology: perspectives and prospects. *J. Clin. Oncol.* **2013**, *31*, 1904-11.
- 5) Fruman, D. A.; Rommel, C. PI3K and cancer: lessons, challenges and opportunities. *Nat. Rev. Drug. Discov.* **2014**, *13*, 140-56.
- 6) Brennan, C. W.; Verhaak, R. G.; McKenna, A.; Campos, B.; Noushmehr, H.; Salama, S. R.; Zheng, S.; Chakravarty, D.; Sanborn, J. Z.; Berman, S. H.; Beroukhim, R.; Bernard, B.; Wu, C. J.; Genovese, G.; Shmulevich, I.; Barnholtz-Sloan, J.; Zou, L.; Vegesna, R.; Shukla, S. A.; Ciriello, G.; Yung, W. K.; Zhang, W.; Sougnez, C.; Mikkelsen, T.; Aldape, K.; Bigner, D. D.; Van Meir, E. G.; Prados, M.; Sloan, A.; Black, K. L.; Eschbacher, J.; Finocchiaro, G.; Friedman, W.; Andrews, D. W.; Guha, A.; Iacocca, M.; O'Neill, B. P.; Foltz, G.; Myers, J.; Weisenberger, D. J.; Penny, R.; Kucherlapati, R.; Perou, C. M.; Hayes, D. N.; Gibbs, R.; Marra, M.; Mills, G. B.; Lander, E.; Spellman, P.; Wilson, R.; Sander, C.; Weinstein, J.; Meyerson, M.; Gabriel, S.; Laird, P. W.; Haussler, D.; Getz, G.; Chin, L.; Network, T. R. The somatic genomic landscape of glioblastoma. *Cell.* **2013**, *155*, 462-77.
- 7) Cloughesy, T. F.; Cavenee, W. K.; Mischel, P. S. Glioblastoma: from molecular pathology to targeted treatment. *Annu. Rev. Pathol.* **2014**, *9*, 1-25.
- 8) Thorpe, L. M.; Yuzugullu, H.; Zhao, J. J. PI3K in cancer: divergent roles of isoforms, modes of activation and therapeutic targeting. *Nat. Rev. Cancer.* **2014**, *15*, 7-24.
- 9) Sonoda, Y.; Ozawa, T.; Hirose, Y.; Aldape, K. D.; McMahon, M.; Berger, M. S.; Pieper, R. O. Formation of intracranial tumors by genetically modified human astrocytes defines four pathways critical in the development of human anaplastic astrocytoma. *Cancer Res.* **2001**, *61*, 4956-60.
- 10) Wen, P. Y.; Lee, E. Q.; Reardon, D. A.; Ligon, K. L.; Alfred; Yung, W. K. Current clinical development of PI3K pathway inhibitors in glioblastoma. *Neuro. Oncol.* **2012**, *14*, 819-29.
- 11) Vanhaesebroeck, B.; Guillermet-Guibert, J.; Graupera, M.; Bilanges, B. The emerging mechanisms of isoform-specific PI3K signaling. *Nat. Rev. Mol. Cell Biol.* **2010**, *11*, 329-41.
- 12) Hanahan, D.; Weinberg, R. A. Hallmarks of cancer: the next generation. *Cell.* **2011**, *144*, 646-74.
- 13) Vadas, O.; Burke, J. E.; Zhang, X.; Berndt, A.; Williams, R. L. Structural basis for activation and inhibition of class I phosphoinositide 3-kinases. *Sci. Signal.* **2011**, *4*, re2.
- 14) Gao, J.; Aksoy, B. A.; Dogrusoz, U.; Dresdner, G.; Gross, B.; Sumer, S. O.; Sun, Y.; Jacobsen, A.; Sinha, R.; Larsson, E.; Cerami, E.; Sander, C.; Schultz, N. Integrative Analysis of Complex Cancer Genomics and Clinical Profiles Using the cBioPortal. **2013**.
- 15) Cerami, E.; Gao, J.; Dogrusoz, U.; Gross, B. E.; Sumer, S. O.; Aksoy, B. A.; Jacobsen, A.; Byrne, C. J.; Heuer, M. L.; Larsson, E.; Antipin, Y.; Reva, B.; Goldberg, A. P.; Sander, C.;

- Schultz, N. The cBio cancer genomics portal: an open platform for exploring multidimensional cancer genomics data. *Cancer Discov.* **2012**, 2, 401-4.
- 16) Koren, S.; Bentires-Alj, M. Mouse models of PIK3CA mutations: one mutation initiates heterogeneous mammary tumors. *FEBS. J.* **2013**, 280, 2758-65.
 - 17) Hanker, A. B.; Pfefferle, A. D.; Balko, J. M.; Kuba, M. G.; Young, C. D.; Sanchez, V.; Sutton, C. R.; Cheng, H.; Perou, C. M.; Zhao, J. J.; Cook, R. S.; Arteaga, C. L. Mutant PIK3CA accelerates HER2-driven transgenic mammary tumors and induces resistance to combinations of anti-HER2 therapies. *Proc. Natl. Acad. Sci.* **2013**, 110, 14372-77.
 - 18) Bader, A. G.; Kang, S.; Vogt, P. K. Cancer-specific mutations in PIK3CA are oncogenic in vivo. *Proc. Natl. Acad. Sci.* **2006**, 103, 1475-79.
 - 19) Zhao, L.; Vogt, P. K. Class I PI3K in oncogenic cellular transformation. *Oncogene.* **2008**, 27, 5486-96.
 - 20) Huang, C. H.; Mandelker, D.; Schmidt-Kittler, O.; Samuels, Y.; Velculescu, V. E.; Kinzler, K. W.; Vogelstein, B.; Gabelli, S. B.; Amzel, L. M. The structure of a human p110alpha/p85alpha complex elucidates the effects of oncogenic PI3Kalpha mutations. *Science.* **2007**, 318, 1744-48.
 - 21) Carson, J. D.; Van Aller, G.; Lehr, R.; Sinnamon, R. H.; Kirkpatrick, R. B.; Auger, K. R.; Dhanak, D.; Copeland, R. A.; Gontarek, R. R.; Tummino, P. J.; Luo, L. Effects of oncogenic p110alpha subunit mutations on the lipid kinase activity of phosphoinositide 3-kinase. *Biochem. J.* **2008**, 409, 519-24.
 - 22) Hon, W. C.; Berndt, A.; Williams, R. L. Regulation of lipid binding underlies the activation mechanism of class IA PI3-kinases. *Oncogene.* **2012**, 31, 3655-66.
 - 23) Gkeka, P.; Evangelidis, T.; Pavlaki, M.; Lazani, V.; Christoforidis, S.; Agianian, B.; Cournia, Z. Investigating the structure and dynamics of the PIK3CA wild-type and H1047R oncogenic mutant. *PLoS Comput. Biol.* **2014**, 10, e1003895.
 - 24) Zhao, L.; Vogt, P. K. Helical domain and kinase domain mutations in p110alpha of phosphatidylinositol 3- kinase induce gain of function by different mechanisms. *Proc. Natl. Acad. Sci.* **2008**, 105, 2652-57.
 - 25) Rich, J. N.; Guo, C.; McLendon, R. E.; Bigner, D. D.; Wang, X. F.; Counter, C. M. A genetically tractable model of human glioma formation. *Cancer Res.* **2001**, 61, 3556-60.
 - 26) Campeau, E.; Ruhl, V. E.; Rodier, F.; Smith, C. L.; Rahmberg, B. L. et al. A Versatile Viral System for Expression and Depletion of Proteins in Mammalian Cells. *PLoS ONE.* **2009**, 4(8), e6529.